



# Toward Real-Time Determination of Yield Coefficients of Early-Stage Electroactive Biofilms by Optical Microscopy

Francesco Scarabotti<sup>1</sup>, Anne Kuchenbuch<sup>1</sup>, René Kallies<sup>1</sup>, Katja Bühler<sup>2</sup> and Falk Harnisch<sup>1\*</sup>

<sup>1</sup>Department of Environmental Microbiology, Helmholtz-Centre for Environmental Research—UFZ, Leipzig, Germany,

<sup>2</sup>Department Solar Materials, Helmholtz-Centre for Environmental Research—UFZ, Leipzig, Germany

Physiological cellular parameters, such as latency times ( $lag_t$ ), cell production rates (CPR), doubling times ( $t_d$ ), relative growth rates (RGR), and yield coefficients ( $Y_{Ne}$ ), are only known as endpoint measurements for electroactive microorganisms (EAM). Here we show that these can be gained non-invasively and in real-time for early-stage biofilm formation at electrodes using a microfluidic electrochemical flow-cell (EFC) allowing *in vivo* optical microscopy. Parameters obtained for early-stage mixed culture biofilm anodes formed at +150 mV vs. Ag/AgCl sat. KCl have  $lag_t$  of 2.31–4.58 days, CPR of  $0.72$ – $1.20 \times 10^5$  cells  $h^{-1}$ ,  $t_d$  of 176.54–1838.65 min, RGR of  $0.02$ – $0.27 h^{-1}$ , and  $Y_{Ne}$  of  $5.99$ – $7.94 \times 10^{12}$  cells  $mol_e^{-1}$ . However, oxygen permeation into the EFC was the main problem that remained unsolved during the study that provides interesting lessons for future improvements.

**Keywords:** electroactive microorganisms, relative growth rates, duplication rate, *Geobacter*, flow-cell

## OPEN ACCESS

### Edited by:

Pierangela Cristiani,  
Ricerca Sul Sistema Energetico, Italy

### Reviewed by:

Xianhua Liu,  
Tianjin University, China  
Olja Simoska,  
The University of Utah, United States

### \*Correspondence:

Falk Harnisch  
falk.harnisch@ufz.de

### Specialty section:

This article was submitted to  
Bioenergy and Biofuels,  
a section of the journal  
Frontiers in Energy Research

**Received:** 14 April 2022

**Accepted:** 24 May 2022

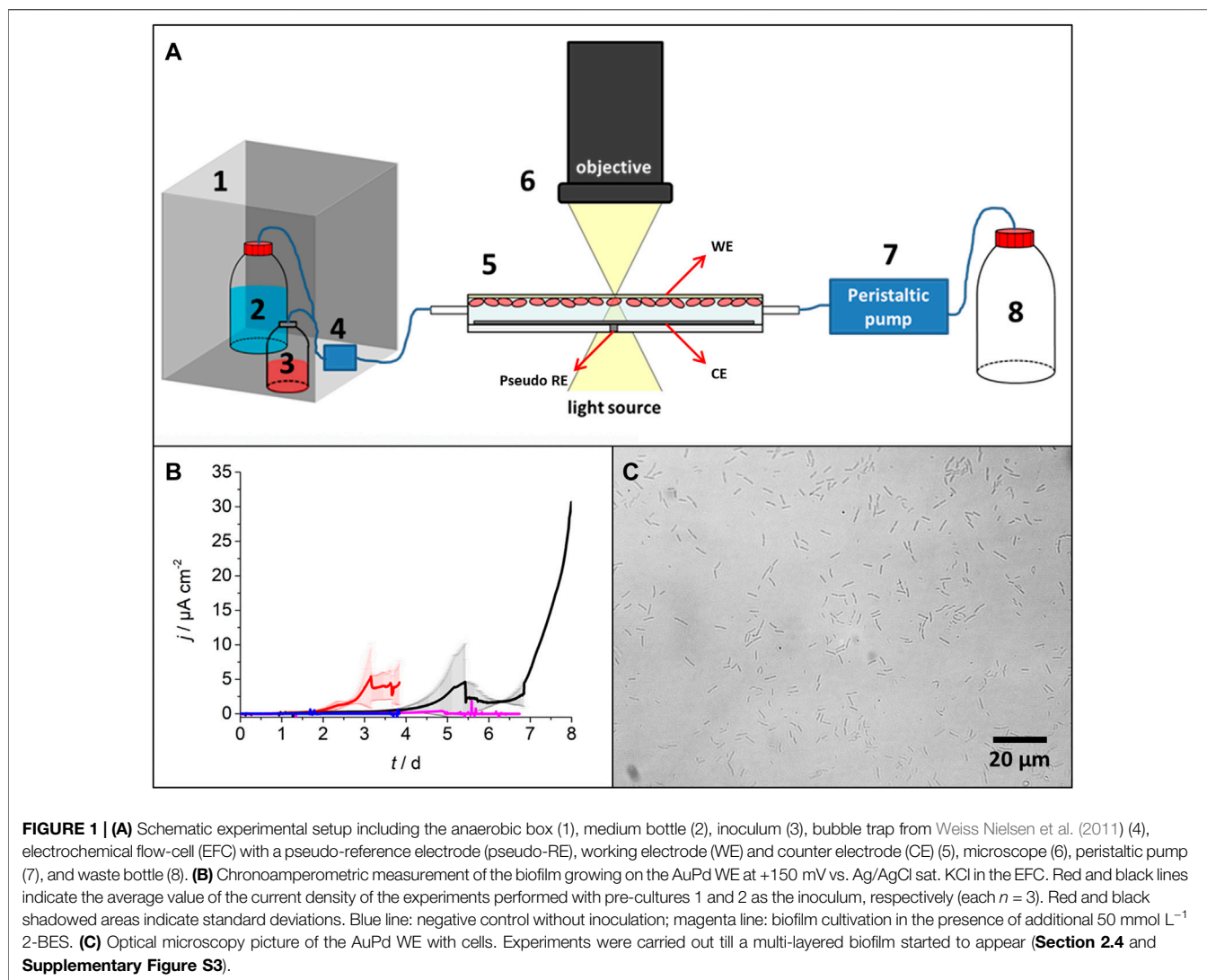
**Published:** 05 July 2022

### Citation:

Scarabotti F, Kuchenbuch A, Kallies R,  
Bühler K and Harnisch F (2022)  
Toward Real-Time Determination of  
Yield Coefficients of Early-Stage  
Electroactive Biofilms by  
Optical Microscopy.  
Front. Energy Res. 10:920266.  
doi: 10.3389/fenrg.2022.920266

## 1 INTRODUCTION

Electroactive microorganisms (EAM) use extracellular electron transfer (EET) to exchange electrons for the metabolism with their environment (Lovley, 2012). Solid-state minerals or electrodes are used as the terminal electron acceptor (TEA), the latter enabling coupling of the EAM metabolism to an external electric circuit. EET can be direct, indirect, or mediated (Lovley, 2012; Ikeda et al., 2021; Lovley and Holmes, 2021). When direct EET is used, a physical contact between the outer membrane cytochromes and the electrode is required resulting in the formation of electroactive biofilms. The model organisms for direct EET are Geobacteraceae that form thick anodic biofilms ( $>100 \mu m$ ) with high electrical conductivity (Lovley, 2012; Lovley and Walker, 2019; Wang et al., 2019), whereas the other model organism *Shewanella* can perform both direct and mediated EET (Baron et al., 2009; Ikeda et al., 2021). EAM find several applications in primary microbial electrochemical technologies (MET) (Schröder, 2011; Logan et al., 2019). The beating heart of all primary MET based on EAM performing direct EET is the electroactive biofilm at the anode. However, there is still a significant lack of knowledge on fundamental physiological properties such as cell production rates (CPR), relative growth rates (RGR), and yield coefficients ( $Y_{Ne}$ ), particularly for mixed culture electroactive biofilms. These kinds of data are highly relevant for fundamental research, for example, as modeling parameters, and set the foundation for prospective bioprocess development. Reported fundamental physiological parameters for EAM were determined either by studying cells growing planktonically on soluble TEA such as fumarate or Fe(III) or on carbon-based electrodes (Brown et al., 2005; Esteve-Nunez et al., 2005; Heidrich



et al., 2016). As polycrystalline carbon or graphite is optically not transparent, markers that allow not only end-point measurements are needed. Recently, using transparent AuPd anodes, we determined latency times ( $lag_t$ ) and  $Y_{Ne}$  for pure-culture early-stage electroactive biofilms of *G. sulfurreducens* (Scarabotti et al., 2021; Scarabotti et al., 2022). This required cell staining for performing confocal laser scanning microscopy (CLSM) for single-cell determination. Thus, only end-point measurements were possible and the biofilms needed to be “sacrificed” for each measurement. Here, we report determining  $lag_t$  and  $Y_{Ne}$  determined using an electrochemical flow-cell (EFC), permitting non-invasive and real-time analysis by optical microscopy for *in vivo* studies.

## 2 MATERIALS AND METHODS

Chemicals of at least analytical grade from Carl Roth GmbH (Karlsruhe, Germany) and Merck KGaA (Darmstadt, Germany)

and de-ionized water (Millipore, Darmstadt, Germany) were used. Provided potentials refer to the Ag/AgCl sat. KCl (+197 mV vs. standard hydrogen electrode, SHE).

### 2.1 Microorganism, Cultivation Media and Pre-culture

Enrichment cultures derived from wastewater inoculum and mainly dominated by *Geobacter anodireducens* served as the inoculum (Gimkiewicz and Harnisch, 2013; Korth et al., 2020a; Korth et al., 2020b). Two pre-cultures (pre-cultures 1 and 2) of two biofilm electrodes in double-chamber four-neck round-bottom flasks, hereafter referred to as electrochemical batch reactors (EBR), were used as the inoculum for all experiments (**Supplementary Section S1.1**).

### 2.2 Electrochemical Flow-Cell

The electrochemical flow-cell (EFC) was custom built based on a standard flow-cell (BioCentrum, Technical University of

Denmark) (Weiss Nielsen et al., 2011), which was modified to host a three-electrode system for the electrochemical cultivation in anaerobic conditions. An Ag/AgCl pseudo-reference electrode (pseudo-RE) (Polk et al., 2006), a titanium wire as the counter electrode (CE), and a transparent AuPd working electrode (WE) (Scarabotti et al., 2021, Scarabotti et al., 2022) were implemented (Figure 1A; for the fabrication procedure, refer Supplementary Sections S3.4–S3.7).

## 2.3 Electrochemical Experiments

Figure 1A shows the experimental setup consisting of an anaerobic box (1) containing the medium bottle (2), the inoculum pre-culture (3), the bubble trap from Weiss Nielsen et al. (2011) (4), the EFC (5), the optical microscope (6) (BH2 Olympus equipped with a 40X air objective and an XC30 camera, Olympus), and the peristaltic pump (7) (4-channel pump, ISMATEC REGLO ICC®). The setup was positioned on a grounded electrostatic mat. An electrostatic bracelet connected to the electrostatic mat and to the ground was worn when handling the experiment. Tubing was generally E-3603 Tygon (ID 1.6 mm, OD 3.2 mm, wall 0.8 mm, ACF00002-C, Saint-Gobain performance plastics, Charny, France); tubing for the peristaltic pump and the tubing located in the anaerobic box were made of silicon or PTFE. All the components and the assembled EFC were sterilized under UV light for at least 2 h, while the silicon/PTFE tubing and the medium bottle were autoclaved. The anaerobic box and the medium bottle were continuously purged with nitrogen gas ( $6 \text{ mL min}^{-1}$ ). Before each experiment, the EFC was flushed with a sterile anaerobic medium for 30 min at  $2.5 \text{ mL min}^{-1}$ . Microscopic pictures on the transparent AuPd WE were taken before inoculation of each experiment to ensure the absence of contamination. Subsequently, the EFC was emptied using nitrogen gas and inoculated with the prepared pre-cultures according to Supplementary Section S1.1. Air bubbles were removed, and the flow rate was set to  $2.5 \mu\text{L min}^{-1}$ . Chronoamperometry (CA) at 0 mV (being +150 mV vs. Ag/AgCl sat. KCl, Supplementary Figure S1, Supplementary Section S3.5) or open-circuit potential (OCP) measurements were applied to the EFC using a potentiostat (SP-200, Biologic®, Claix, France) equipped with an ultra-low current detection module. After 24 h of continuous inoculation, a sterile fresh medium supplemented with  $5 \text{ mmol L}^{-1}$  acetate was continuously pumped through the EFC. For some experiments, an additional  $50 \text{ mmol L}^{-1}$  of 2-BES (2-bromoethanesulfonate) was added to prevent the growth of archaea (Kosse et al., 2016; Webster et al., 2016). As control experiments, chronoamperometric cultivation at +150 mV vs. Ag/AgCl sat. KCl and OCP were performed in the EBR.

## 2.4 Microscopy Pictures Analysis

Per each time point, ten pictures were acquired (five pictures on the left and right of the WE, respectively; Supplementary Figure S2). The pictures were analyzed (ImageJ 1.45 s, Java 1.8.0\_202, 32-bit) for cell counting. Cell counting was possible till a multilayer biofilm started to appear (Supplementary Section S1.2; Supplementary Figures S3, S4).

## 2.5 Sampling and Microbial Community Analysis

The inoculum was sampled before each experiment (Supplementary Section S1.1), while the biofilms of the EFC and EBR were sampled at the end of each experiment under sterile conditions. Genomic DNA was extracted, and PCR and amplicon sequencing of the bacterial 16S rRNA gene and archaeal *mcrA* gene were performed (Supplementary Sections S1.3, S1.4).

## 2.6 Calculations of Latency Times, Relative Growth Rates, Cell Production Rates, Doubling Times, and Yield Coefficients

In line with Scarabotti et al. (2021) and Scarabotti et al. (2022),  $lag_t$  was defined as the time from inoculation until  $j \geq 1 \mu\text{A cm}^{-2}$ . The cell number ( $N_{\text{cell}}$ ) at a time point  $t$  was obtained via microscopy (Section 2.4 and Supplementary Section S1.2) and correlated to the charge to calculate the CPR (Eq. 1),  $t_d$  (Eq. 2), RGR (Eq. 3), and  $Y_{Ne}$  expressed in cells  $\text{mol}_e^{-1}$  (Eq. 4) (Koch and Harnisch, 2016; Scarabotti et al., 2021; Scarabotti et al., 2022).

$$CPR = \text{slope}, \quad (1)$$

with the slope being the angular coefficient of the linear regression from data points plotted with time ( $t$ ,  $x$ -axis) and number of cells ( $N_{\text{cell}}$ ,  $y$ -axis).

$$t_d = \frac{\ln(2)}{\ln(1 + RGR)} \quad (2)$$

$$RGR = \frac{\ln(N_{\text{cell}, t_2}) - \ln(N_{\text{cell}, t_1})}{t_2 - t_1} \quad (3)$$

with  $N_{\text{cell}, t_2}$  and  $N_{\text{cell}, t_1}$  being the number of cells counted at  $t_2$  and  $t_1$ , respectively. The RGRs were calculated independently for pre-cultures 1 and 2 (Section 2.1).

$$Y_{Ne} = \text{slope} \times F, \quad (4)$$

with the slope being the angular coefficient of the linear regression on data points plotted as the measured charge ( $Q$ ,  $x$ -axis) versus the cell number ( $N_{\text{cell}}$ ,  $y$ -axis) and  $F$  as the Faraday constant ( $96,485 \text{ C mol}_e^{-1}$ ).

## 3 RESULTS AND DISCUSSION

### 3.1 Chronoamperometric Cultivation and Determination of Relative Growth Rates, Doubling Times, and Yield Coefficients

Figure 1B shows the chronoamperometric cultivation of electroactive biofilms in the EFC on AuPd WE at +150 mV vs. Ag/AgCl sat. KCl. The current profiles based on pre-cultures 1 and 2 were similar, but their latency differed significantly. For pre-culture 1,  $lag_t$  was  $2.31 \pm 0.20$  days ( $n = 3$ ), whereas for pre-culture 2,  $lag_t$  was  $4.58 \pm 1.14$  days ( $n = 3$ ). Thus,  $lag_t$  are in accordance with our previous studies (Scarabotti et al., 2021; Scarabotti et al., 2022) for  $G$ .

**TABLE 1** | Latency time (*lag*t), relative growth rates (RGR), cell production rate (CPR), doubling times (*t*<sub>d</sub>), and yield coefficients (*Y*<sub>Ne</sub>) of early-stage mixed culture electroactive biofilms.

		Inoculum	Anode material/electron acceptor	E/mV	<i>lag</i> t/d	Flow rate/ $\mu\text{L min}^{-1}$				
One-chamber electrochemical flow-cell (EFC) with potentiostatic control										
1	Pre-culture 1	Mixed culture	AuPd <sup>b</sup>	+150 <sup>a</sup>	2.31 ± 0.20 ( <i>n</i> = 3)	2.5				
2	Pre-culture 2	Mixed culture	AuPd <sup>b</sup>	+150 <sup>a</sup>	4.58 ± 1.14 ( <i>n</i> = 3) <sup>c</sup>	2.5				
Batch reactors with potentiostatic control										
3	One-chamber	<i>G. sulfurreducens</i>	AuPd <sup>b</sup>	+200 <sup>a</sup>	5.32 ± 1.82 ( <i>n</i> = 5)	n. a.				
4	Two-chamber	<i>G. sulfurreducens</i>	AuPd <sup>b</sup>	-200 <sup>a</sup>	0.24 ± 0.26 ( <i>n</i> = 7)	n. a.				
5	Two-chamber	<i>G. sulfurreducens</i>	Graphite	+200 <sup>a</sup>	0.05 ± 0.03 ( <i>n</i> = 3)	n. a.				
Other										
6	MFC two-chamber	<i>S. oneidensis</i> MR-1	Pure carbon fiber veil	/	/	130–1,200 <sup>d</sup>				
7	Chemostat	<i>G. sulfurreducens</i>	Fumarate Fe (III)	/	/	n. a.				
8	MFC two-chamber	Wastewater-fed community Starch-fed community Acetate-fed electrogen	Carbon felt	/	//	n. a.				
9	—	<i>G. sulfurreducens</i> / <i>W. succinogenes</i> <i>G. sulfurreducens</i> / <i>D. desulfuricans</i>	Nitrate sulfide	/	/	n. a.				
	RGR/h <sup>-1</sup>	$\mu_{\text{max}}$ /h <sup>-1</sup>	CPR/cells h <sup>-1</sup>	<i>r</i>	Adj. R2	<i>t</i> <sub>d</sub> /min	<i>Y</i> <sub>Ne</sub> /cells mol <sub>e</sub> <sup>-1</sup>	<i>r</i>	Adj. R2	Ref.
One-chamber electrochemical flow-cell (EFC) with potentiostatic control										
1	0.02 ± 0.62	/	1.20 × 10 <sup>5</sup> ± 6.43 × 10 <sup>3</sup>	0.96	0.92	1838.65 ± 86.04	5.99 × 10 <sup>12</sup> ± 1.34 × 10 <sup>12</sup>	0.64	0.39	This study
2	0.27 ± 0.97	/	7.21 × 10 <sup>4</sup> ± 7.10 × 10 <sup>3</sup>	0.95	0.89	176.54 ± 61.39	7.94 × 10 <sup>12</sup> ± 1.41 × 10 <sup>12</sup>	0.86	0.72	This study
Batch reactors with potentiostatic control										
3	/	/	/	/	/	/	2.58 × 10 <sup>11</sup> ± 8.04 × 10 <sup>10</sup>	0.88	0.7	Scarabotti et al. (2021)
4	/	/	/	/	/	/	1.43 × 10 <sup>12</sup> ± 1.52 × 10 <sup>11</sup>	0.86	0.73	Scarabotti et al. (2022)
5	/	/	/	/	/	/	/	/	/	Scarabotti et al. (2021)
Other										
6	0.17–0.67	/	/	/	/	/	/	/	/	Greenman et al. (2011)
7	0.04–0.09	0.15 ± 0.01	/	/	/	/	/	/	/	Esteve-Nunez et al. (2005)
8	0.028 ± 0.013	0.023 ± 0.005	/	/	/	/	/	/	//	Heidrich et al. (2016)
9	0.099	0.023	/	/	/	/	/	/	/	Cord-Ruwisch, Lovley and Schink (1998)

/: Indicates that the information is neither stated nor clear from the manuscript or not determined; n. a.: Not applicable.

<sup>a</sup>Potential values are converted to vs. Ag/AgCl sat. KCl.

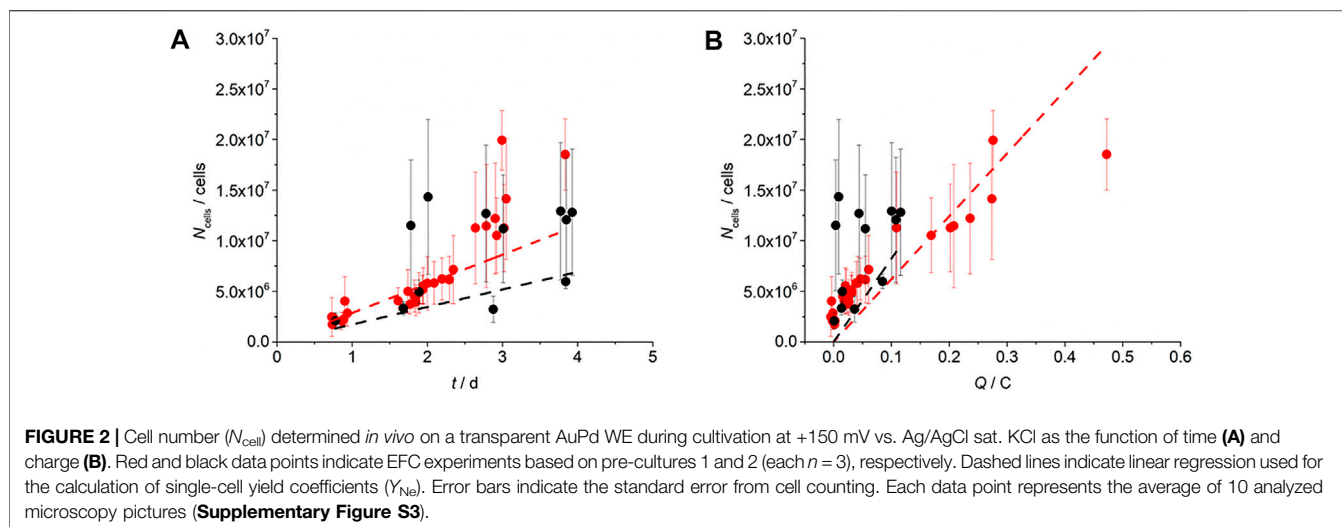
<sup>b</sup>Electrode thickness of 25 nm.

<sup>c</sup>One of the replicates did not reach the current density of 1  $\mu\text{A cm}^{-2}$ , but 0.7  $\mu\text{A cm}^{-2}$ .

<sup>d</sup>Value converted from original units.

*sulfurreducens* cultured in single- or double-chamber reactors on the AuPd WE (Table 1). Only at -200 mV vs. Ag/AgCl sat. KCl in double-chamber reactors *G. sulfurreducens* did show a lower *lag*t of 0.24 ± 0.26 days (*n* = 7). The shortest *lag*t of 0.05 ± 0.03 days (*n* = 3) was observed for biofilms on graphite anodes at +200 mV vs. Ag/AgCl sat. KCl in double-chamber reactors, which can be assigned to the different electrode materials (Table 1). Differences in latency

were also observed by other researchers and might reflect the intrinsic heterogeneity in the microbial communities and the stochasticity of the initial settling phase during biofilm formation (Molenaar et al., 2018). The 16S rRNA gene sequencing data (Supplementary Section S1.3) show that the bacterial community composition of the biofilms in the EFC strongly differs from the inoculum.



Non-invasive optical microscopy for determining  $N_{\text{cell}}$  of the AuPd WE (**Figure 2A**) showed an increase in the  $N_{\text{cell}}$  with the cultivation time for all CA experiments. To confirm microbial electrochemical activity, an abiotic control was performed showing no current production after 92 h (**Figure 1B**, blue line). For OCP controls, where the electric circuit was opened and thus the WE did not serve as TEA, a 24.4% increase was observed (**Supplementary Figure S5**). This was also the case in the presence of  $50 \text{ mmol L}^{-1}$  2-BES, being an inhibitor of archaea, where also no current was observed (**Figure 1B**). One may speculate that this non-electrochemical microbial growth decreases during electrochemical cultivation.

The high standard errors in the  $N_{\text{cell}}$  can be assigned to an inhomogeneous cell distribution over the AuPd WE during early-stage biofilm formation. As **Supplementary Figure S6** shows, a higher cell density was observed closer to the inflow of the EFC. We hypothesize that this is mainly due to a voltage drop ( $i \times R$  drop) over the length of the anode (**Supplementary Figure S7**). **Figures 2A,B** show the determination of the physiological parameters of the early-stage electroactive biofilms, with a CPR of  $1.20 \times 10^5 \text{ cells h}^{-1}$  and  $7.21 \times 10^4 \text{ cells h}^{-1}$ ,  $t_d$  of  $1838.65 \pm 86.04 \text{ min}$  and  $176.54 \pm 61.39 \text{ min}$ , and the RGR being  $0.02 \pm 0.62 \text{ h}^{-1}$  and  $0.27 \pm 0.97 \text{ h}^{-1}$ , for the EFC based on pre-cultures 1 and 2, respectively (**Table 1**). Esteve-Nunez et al. (2005) showed that pure cultures of *G. sulfurreducens* grown on soluble TEA fumarate and Fe(III) exhibited an RGR of  $0.04\text{--}0.09 \text{ h}^{-1}$ , with maximum growth rates of  $0.15 \pm 0.01 \text{ h}^{-1}$  and  $0.1 \pm 0.01 \text{ h}^{-1}$ , respectively. Similarly, Heidrich et al. (2016) reported for wastewater, acetate, or starch-fed communities RGR of  $0.028 \pm 0.013 \text{ h}^{-1}$ ,  $0.023 \pm 0.005 \text{ h}^{-1}$ , and  $0.35 \pm 0.020 \text{ h}^{-1}$ , respectively.

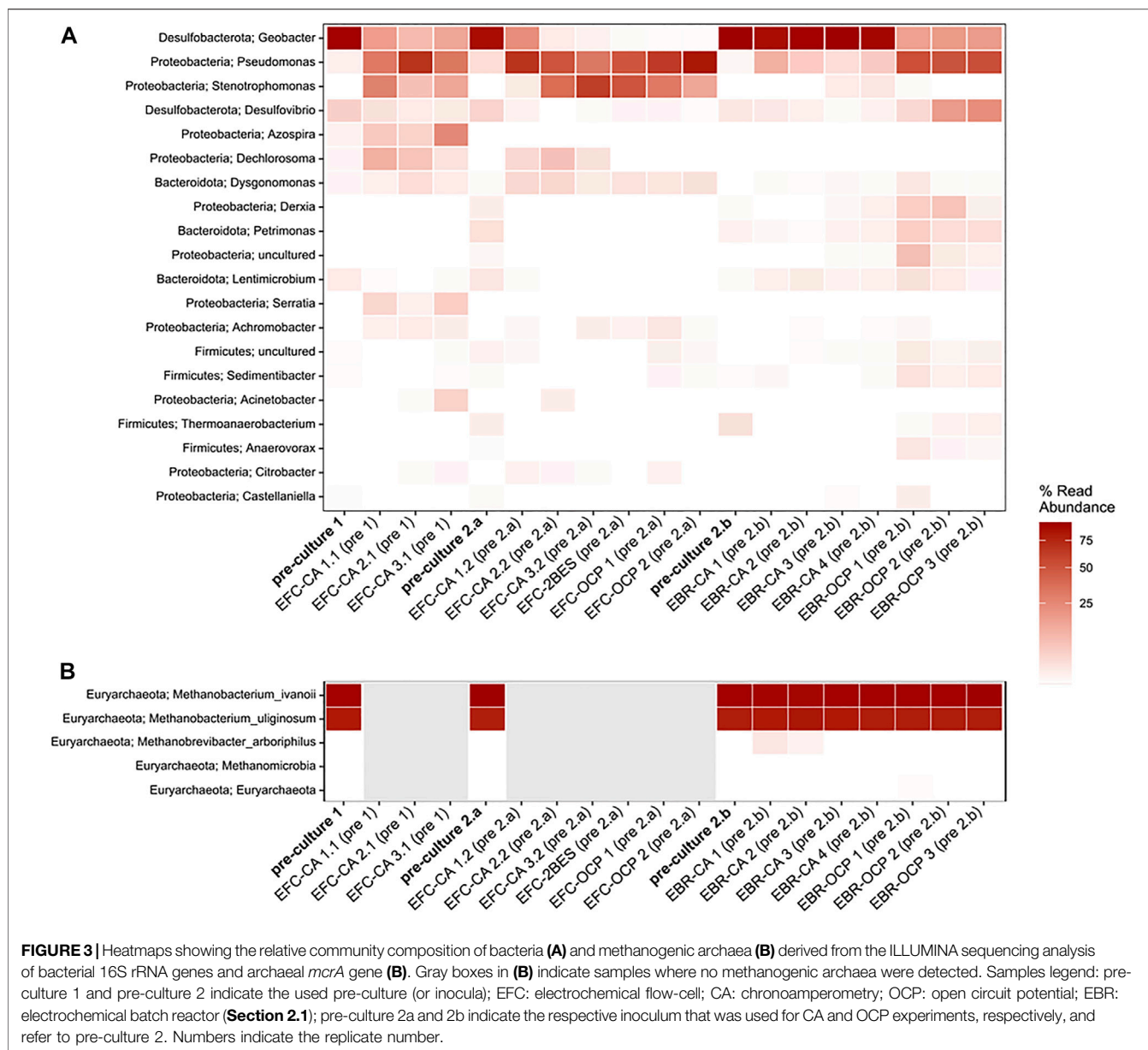
As expected, **Figure 2B** shows an increase in the cell number with charge (Molenaar et al., 2018; Scarabotti et al., 2021; Scarabotti et al., 2022). The  $Y_{\text{Ne}}$  obtained in this study are in the same order of magnitude as in previous studies on early-stage biofilms of *G. sulfurreducens* (Scarabotti et al., 2021;

Scarabotti et al., 2022) (**Table 1**). Furthermore, they are comparable when using different TEA than when using electrodes. For instance, Brown et al. (2005) reported  $Y_{\text{Ne}}$  for *G. sulfurreducens* growing on acetate or hydrogen as electron donors and Fe(III) as the electron acceptor of  $11.03 \times 10^9 \text{ cells mmol}_{\text{acetate}}^{-1}$  and  $16.3 \times 10^9 \text{ cells mmol}_{\text{hydrogen}}^{-1}$ , which is equal to  $1.38 \times 10^{12} \text{ cells mol}_e^{-1}$  and  $8.15 \times 10^{12} \text{ cells mol}_e^{-1}$ , respectively.

### 3.2 Microbial Community Composition

Sequencing of partial bacterial 16S rRNA genes and *mcrA* as the marker gene for methanogenic archaea was applied to analyse the microbial community composition of the pre-cultures and grown biofilms at the end of each experiment. As **Figure 3** shows, both pre-cultures were mainly dominated by the genus *Geobacter* with relative abundances of 91.4 and 85.9%. Interestingly, in all EFC experiments, a community shift was observed. The relative abundances of *Geobacter* decreased toward the end of each experiment to  $13.2 \pm 3.5\%$  for EFC experiments based on pre-culture 1 and  $8.1 \pm 10.3\%$  for EFC experiments based on pre-culture 2. The high standard deviations, especially in the latter case, show that a stable establishment of *Geobacter* was not possible. The presence of other microorganisms, in particular *Pseudomonadaceae*, *Xanthomonadaceae*, and *Rhodocyclaceae*, strongly indicates that the EFC was not maintained under full anaerobic conditions. However, it is worth noticing that in OCP experiments performed in the EFC, *Geobacter* was almost absent in the biofilm samples and a high relative abundance of *Pseudomonadaceae* ( $72.7 \pm 10.1\%$ ) and *Xanthomonadaceae* ( $22.4 \pm 8.3\%$ ) was observed. These results confirm that the presence of an anode as the sole TEA is needed for the growth of electroactive biofilms and particularly *Geobacteraceae*.

Interestingly, *Geobacter* was only present in low proportions (0.2%) in the presence of 2-BES. As expected, in this case, no archaea were detected in the biofilm. Furthermore, neither current nor a significant  $N_{\text{cell}}$  increase



was observed under these conditions (**Figure 1B**, **Supplementary Figure S5**). It was recently shown that the presence of archaea, and in particular, methanogens, in an electroactive biofilm inhibits *Geobacter* activity (Dzoufou et al., 2021). These results are in contradiction with our observations, albeit being based on, for example, a different anode material. More importantly, we have to assume that our system was not anaerobic, as indicated by the presence of aerophilic microorganisms such as *Pseudomonadaceae*, which may explain these differences. Interestingly, for all the CA and OCP EFC experiments, no methanogenic archaea were detected in the biofilms, although they were present in the inoculum. This indicates that an establishment of methanogenic archaea in the EFC was not possible; especially as in OCP controls in the EBR, methanogenic

archaea (in particular, representatives of the hydrogenotrophic *Methanobacteriaceae*) were detected. This observation emphasizes that in the EFC experiments, oxygen could permeate into the system. It should be noted that without microbial community analysis, this shortcoming certainly would have been overlooked and may have led to wrong conclusions. That it is a specific shortcoming of the EFC is also underlined by the CA control experiments in the EBR (**Figure 3**), where anaerobic conditions were maintained and the gained biofilms were dominated by *Geobacter* (up to  $90.2 \pm 3.1\%$ ). The electrochemical data have already indicated this, as in the biotic OCP EBR control experiments (**Supplementary Figure S8**, continuous red line), the potential of the AuPd WE stabilized at  $\sim -400$  to  $500$  mV after  $\sim 24$ – $26$  h of cultivation, whereas in the EFC

experiments, the levels were  $\sim +150$  mV (Supplementary Figure S8, dotted und dashed red lines).

## 4 CONCLUSION

Coupling optical microscopy with chronoamperometric measurements in an EFC allows the correlation of the cell number with time and charge for early-stage electroactive biofilm anodes. This allows obtaining physiological information including replication rates, relative growth rates, and yield coefficients that are needed for process modeling, development, and especially scaling. The introduced EFC shows that the growth of EAM can be monitored *in vivo* in real-time and nondestructively, being a clear advantage when compared with other analyses (e.g., CLSM requiring staining and SEM) requiring sample preparation. The presented EFC is certainly a good starting point for this kind of analysis. Yet, the gathered data are only preliminary and have to be interpreted with outstanding care, and obtaining conclusive data requires significant improvements, especially to work in strictly anaerobic conditions, for example, by housing the entire system in an anaerobic tent. In this endeavor, numerous lessons can be learned from this study.

## DATA AVAILABILITY STATEMENT

Raw sequence data for this study was deposited at the European Nucleotide Archive (ENA) under the study accession number PRJEB52487 (<http://www.ebi.ac.uk/ena/data/view/PRJEB52487>).

## REFERENCES

- Baron, D., LaBelle, E., Coursolle, D., Gralnick, J. A., and Bond, D. R. (2009). Electrochemical Measurement of Electron Transfer Kinetics by *Shewanella Oneidensis* MR-1. *J. Biol. Chem.* 284 (42), 28865–28873. doi:10.1074/jbc.M109.043455
- Brown, D. G., Komlos, J., and Jaffé, P. R. (2005). Simultaneous Utilization of Acetate and Hydrogen by *Geobacter Sulfurreducens* and Implications for Use of Hydrogen as an Indicator of Redox Conditions. *Environ. Sci. Technol.* 39 (9), 3069–3076. doi:10.1021/es048613p
- Cord-Ruwisch, R., Lovley, D. R., and Schink, B. (1998). Growth of *Geobacter Sulfurreducens* with Acetate in Syntrophic Cooperation with Hydrogen-Oxidizing Anaerobic Partners. *Appl. Environ. Microbiol.* 64 (6), 2232–2236. doi:10.1128/AEM.64.6.2232-2236.1998
- Dzofou Ngoumelah, D., Harnisch, F., and Kretzschmar, J. (2021). Benefits of Age-Improved Resistance of Mature Electroactive Biofilm Anodes in Anaerobic Digestion. *Environ. Sci. Technol.* 55 (12), 8258–8266. doi:10.1021/acs.est.0c07320
- Esteve-Nunez, A., Rothermich, M., Sharma, M., and Lovley, D. (2005). Growth of *Geobacter Sulfurreducens* under Nutrient-Limiting Conditions in Continuous Culture. *Environ. Microbiol.* 7 (5), 641–648. doi:10.1111/j.1462-2920.2005.00731.x
- Gimkiewicz, C., and Harnisch, F. (2013). Waste Water Derived Electroactive Microbial Biofilms: Growth, Maintenance, and Basic Characterization. *JoVE* (82), e50800. doi:10.3791/50800
- Greenman, J., Pablo, L., Pereira-Medrano, A. G., Wright, P. C., and Ieropoulos, I. (2011). “The Importance of Specific Growth Rate of Biofilms for Electricity

## AUTHOR CONTRIBUTIONS

FS, FH, and KB contributed to the conception and design of the study. FS performed the experiments and wrote the first draft of the manuscript. AK and RK performed the ILLUMINA sequencing and sequencing analysis. All authors contributed to manuscript revision, and read and approved the submitted version.

## FUNDING

This work was supported by the Helmholtz Association within the Research Programme Renewable Energies.

## ACKNOWLEDGMENTS

We thank Christin Koch for the highly valuable pre-work and discussion. The authors are grateful for the use of the sputter-coater facility at ProVIS-Centre for Chemical Microscopy by the Helmholtz-Centre for Environmental Research, Leipzig, which is supported by the European Regional Development Fund (ERDF, operational programme for Saxony) and the Helmholtz Association.

## SUPPLEMENTARY MATERIAL

The Supplementary Material for this article can be found online at: <https://www.frontiersin.org/articles/10.3389/fenrg.2022.920266/full#supplementary-material>

- Production in Microbial Fuel Cell Systems,” in Proceedings of the IWA Biofilm conference, Shanghai, China, October 2011.
- Heidrich, E. S., Curtis, T. P., Woodcock, S., and Doling, J. (2016). Quantification of Effective Exoelectrogens by Most Probable Number (MPN) in a Microbial Fuel Cell. *Bioresour. Technol.* 218, 27–30. doi:10.1016/j.biortech.2016.06.066
- Ikeda, S., Takamatsu, Y., Tsuchiya, M., Suga, K., Tanaka, Y., Kouzuma, A., et al. (2021). *Shewanella Oneidensis* MR-1 as a Bacterial Platform for Electro-Biotechnology. *Essays Biochem.* 65 (2), 355–364. doi:10.1042/EBC20200178
- Koch, C., and Harnisch, F. (2016). What Is the Essence of Microbial Electroactivity? *Front. Microbiol.* 7 (NOV), 1890. doi:10.3389/fmicb.2016.01890
- Korth, B., Kretzschmar, J., Bartz, M., Kuchenbuch, A., and Harnisch, F. (2020a). Determining Incremental Coulombic Efficiency and Physiological Parameters of Early Stage *Geobacter* Spp. Enrichment Biofilms. *PLOS ONE* 15 (6), e0234077. doi:10.1371/journal.pone.0234077
- Korth, B., Kuchenbuch, A., and Harnisch, F. (2020b). Availability of Hydrogen Shapes the Microbial Abundance in Biofilm Anodes Based on *Geobacter* Enrichment. *ChemElectroChem* 7 (18), 3720–3724. doi:10.1002/celec.202000731
- Kosse, P., Lübken, M., and Wichern, M. (2016). Selective Inhibition of Methanogenic Archaea in Leach Bed Systems by Sodium 2-bromoethanesulfonate. *Environ. Technol. Innovation* 5, 199–207. doi:10.1016/j.eti.2016.03.003
- Logan, B. E., Rossi, R., Ragab, A. a., and Saikaly, P. E. (2019). Electroactive Microorganisms in Bioelectrochemical Systems. *Nat. Rev. Microbiol.* 17 (5), 307–319. doi:10.1038/s41579-019-0173-x
- Lovley, D. R. (2012). Electromicrobiology. *Annu. Rev. Microbiol.* 66 (1), 391–409. doi:10.1146/annurev-micro-092611-150104

- Lovley, D. R., and Holmes, D. E. (2021). Electromicrobiology: the Ecophysiology of Phylogenetically Diverse Electroactive Microorganisms. *Nat. Rev. Microbiol.* 20, 5–19. doi:10.1038/s41579-021-00597-6
- Lovley, D. R., and Walker, D. J. F. (2019). Geobacter Protein Nanowires. *Front. Microbiol.* 10. doi:10.3389/fmicb.2019.02078
- Molenaar, S. D., Sluets, T., Pereira, J., Iorio, M., Borsje, C., Zamudio, J. A., et al. (2018). *In Situ* Biofilm Quantification in Bioelectrochemical Systems by Using Optical Coherence Tomography. *ChemSusChem* 11 (13), 2171–2178. doi:10.1002/cssc.201800589
- Polk, B. J., Stelzenmuller, A., Mijares, G., MacCrehan, W., and Gaitan, M. (2006). Ag/AgCl Microelectrodes with Improved Stability for Microfluidics. *Sensors Actuators B Chem.* 114 (1), 239–247. doi:10.1016/j.snb.2005.03.121
- Scarabotti, F., Bühler, K., Schmidt, M., and Harnisch, F. (2022). Thickness and Roughness of Transparent Gold-Palladium Anodes Have No Impact on Growth Kinetics and Yield Coefficients of Early-Stage Geobacter Sulfurreducens Biofilms. *Bioelectrochemistry* 144, 108043. doi:10.1016/j.bioelechem.2021.108043
- Scarabotti, F., Rago, L., Bühler, K., and Harnisch, F. (2021). The Electrode Potential Determines the Yield Coefficients of Early-Stage Geobacter Sulfurreducens Biofilm Anodes. *Bioelectrochemistry* 140, 107752. doi:10.1016/j.bioelechem.2021.107752
- Schröder, U. (2011). Discover the Possibilities: Microbial Bioelectrochemical Systems and the Revival of a 100-Year-Old Discovery. *J. Solid State Electrochem* 15, 1481–1486. doi:10.1007/s10008-011-1395-7
- Wang, F., Gu, Y., O'Brien, J. P., Yi, S. M., Yalcin, S. E., Srikanth, V., et al. (2019). Structure of Microbial Nanowires Reveals Stacked Hemes that Transport Electrons over Micrometers. *Cell.* 177 (2), 361–369. e10. doi:10.1016/j.cell.2019.03.029
- Webster, T. M., Smith, A. L., Reddy, R. R., Pinto, A. J., Hayes, K. F., and Raskin, L. (2016). Anaerobic Microbial Community Response to Methanogenic Inhibitors 2-bromoethanesulfonate and Propynoic Acid. *MicrobiologyOpen* 5 (4), 537–550. doi:10.1002/mbo3.349
- Weiss Nielsen, M., Sternberg, C., Molin, S., and Regenber, B. (2011). *Pseudomonas aeruginosa* and *Saccharomyces cerevisiae* Biofilm in Flow Cells. *JoVE* (47), 2383. doi:10.3791/2383
- Conflict of Interest:** The authors declare that the research was conducted in the absence of any commercial or financial relationships that could be construed as a potential conflict of interest.
- Publisher's Note:** All claims expressed in this article are solely those of the authors and do not necessarily represent those of their affiliated organizations, or those of the publisher, the editors, and the reviewers. Any product that may be evaluated in this article, or claim that may be made by its manufacturer, is not guaranteed or endorsed by the publisher.
- Copyright © 2022 Scarabotti, Kuchenbuch, Kallies, Bühler and Harnisch. This is an open-access article distributed under the terms of the Creative Commons Attribution License (CC BY). The use, distribution or reproduction in other forums is permitted, provided the original author(s) and the copyright owner(s) are credited and that the original publication in this journal is cited, in accordance with accepted academic practice. No use, distribution or reproduction is permitted which does not comply with these terms.